LETTERS

STING is an endoplasmic reticulum adaptor that facilitates innate immune signalling

Hiroki Ishikawa[1] & Glen N. Barber[1]

The cellular innate immune system is essential for recognizing pathogen infection and for establishing effective host defence. But critical molecular determinants responsible for facilitating an appropriate immune response—following infection with DNA and RNA viruses, for example—remain to be identified. Here we report the identification, following expression cloning, of a molecule (STING; stimulator of interferon genes) that appears essential for effective innate immune signalling processes. It comprises five putative transmembrane regions, predominantly resides in the endoplasmic reticulum and is able to activate both NF-κB and IRF3 transcription pathways to induce expression of type I interferon (IFN-α and IFN-β) and exert a potent anti-viral state following expression. In contrast, loss of STING rendered murine embryonic fibroblasts extremely susceptible to negative-stranded virus infection, including vesicular stomatitis virus. Further, STING ablation abrogated the ability of intracellular B-form DNA, as well as members of the herpesvirus family, to induce IFN-β, but did not significantly affect the Toll-like receptor (TLR) pathway. Yeast two-hybrid and co-immunoprecipitation studies indicated that STING interacts with RIG-I and with SSR2 (also known as TRAPβ), which is a member of the translocon-associated protein (TRAP) complex required for protein translocation across the endoplasmic reticulum membrane following translation[1,2]. Ablation by RNA interference of both TRAPβ and translocon adaptor SEC61β was subsequently found to inhibit STING's ability to stimulate expression of IFN-β. Thus, as well as identifying a regulator of innate immune signalling, our results imply a potential role for the translocon in innate signalling pathways activated by select viruses as well as intracellular DNA.

Cellular host defence responses to pathogen invasion principally involve the detection of pathogen associated molecular patterns (PAMPs), such as viral nucleic acid or bacterial cell wall components (including lipopolysaccharide or flagellar proteins), that results in the induction of anti-pathogen genes[3–9]. For example, viral RNA can be detected by membrane bound TLRs present in the endoplasmic reticulum (ER) and/or endosomes (for example, TLR3 and TLR7/8) or by TLR-independent intracellular DExD/H box RNA helicases, referred to as retinoic acid inducible gene 1 (RIG-I) or melanoma differentiation associated antigen 5 (MDA5, also referred to as IFIH1 and helicard)[3–10]. Pathogen DNA can be recognized by TLR9 present in plasmacytoid dendritic cells, although it is now apparent that important TLR-independent pathways also exist to recognize DNA in alternative tissue, the mechanisms of action of which remain to be determined[3–10]. These events culminate in the activation of downstream signalling events, leading to the transcription of NF-κB and IRF3/7-dependent genes, including type I IFN.

To further determine the mechanisms of innate immune signalling, we employed an expression screening system in which approximately 5,500 human and 9,000 murine full length complementary DNAs were individually transfected into 293T cells harbouring a luciferase gene under control of the IFN-β promoter (IFN-β-Luc). The top five hits whose overexpression lead to the significant induction of IFN-β-Luc were found to be IPS-1 (also referred to as VISA/CARDIF/MAVS) (Supplementary Fig. 1)[11–14]. However, we also isolated a previously uncharacterized molecule (gi:38093659/NP_938023/2610307O08RIK) which we referred to as STING that harboured five predicted transmembrane motifs (in humans) and existed as a 379 amino acid protein in human cells and 378 amino acids in murine cells (Fig. 1a and Supplementary Fig. 1). A putative signal cleavage motif was found to exist at position 1–36 and a leucine rich region was apparent between amino acids 21 and 139 (Fig. 1 a). The predicted molecular weight of human STING was 42,192 Da, which approximately corresponded to its observed molecular weight in human 293 cells following immunoblot analysis using a rabbit antiserum raised to a STING peptide (Fig. 1 b). RNAi studies confirmed that the observed 42 kDa band was indeed STING (Fig. 1b). STING was found to be ubiquitously expressed in a variety of tissues, as determined by northern analysis, and was found to predominantly reside in the ER region of the cell as determined by confocal microscopy and fractionation analysis (Fig. 1 c–e).

Overexpression of STING in 293T cells was subsequently confirmed to robustly induce the expression of the IFN promoter (IFN-β-Luc) by up to 400-fold, but not a control TK promoter driving luciferase (pRL-TK), interferon regulatory factor 3 (IRF3) responsive promoters (PRD-III-I-Luc) up to 1,000-fold, an NF-κB responsive promoter (NF-κB-Luc) 12-fold, and interferon-inducible promoters (interferon sensitive response element, ISRE-Luc) up to 800-fold (Fig. 2 a–d). STING did not activate control promoters driving luciferase reporters such as those derived from the RB, p53 or E2F genes (Supplementary Fig. 2). Increased dimerization of IRF3 was also observed in STING expressing 293T cells, confirming that STING regulates the induction of type I IFN at locations upstream of IRF3 activation, dimerization and translocation (Supplementary Fig. 2)[15]. Endogenous *Ifnb* mRNA and IFN-β protein was induced significantly in murine embryonic fibroblasts (MEFs) transiently transfected with STING (Fig. 2e, f). DNA microarray analysis of STING expression in 293T cells further emphasized STING's ability to induce primary innate immune response genes (Fig. 2g). Accordingly, MEF cells expressing STING or IPS-1 were significantly resistant to vesicular stomatitis virus (VSV) infection (Fig. 2h, i). Subsequent analysis indicated that STING function was ablated in the absence of the IκB kinase family member TBK-1, confirming that STING's activity involved activation of IRF3 and was indeed upstream of this kinase (Fig. 2 j)[15]. Finally, we observed that STING did not exert robust activity in the absence of FADD, which has also been shown to be important for efficient innate immune signalling processes (Supplementary Fig. 2)[16].

[1]Department of Medicine and Sylvester Comprehensive Cancer Center, University of Miami School of Medicine, Miami, Florida 33136, USA.

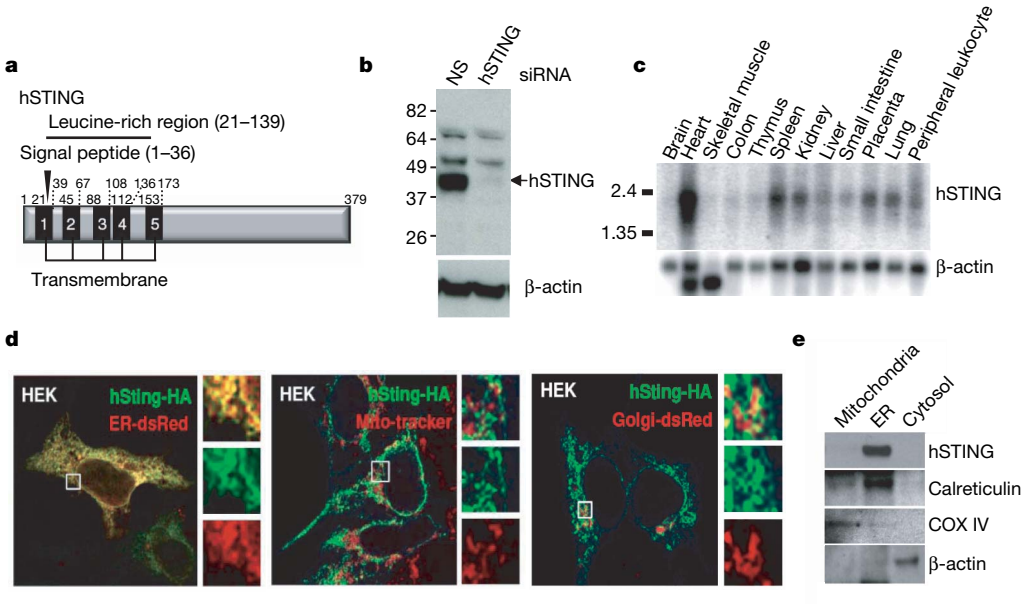

Figure 1 | STING is an ER protein. a, Schematic of human STING (hSTING) indicating transmembrane and leucine rich regions. **b**, Immunoblot analysis of STING in HEK 293 cells treated with RNAi to STING (hSTING) or control RNAi (NS). **c**, Northern blot analysis of human STING and control β-actin. **d**, Confocal analysis of HEK 293 cells (HEK) transfected with human STING tagged at the carboxyl end with HA. Transfected cells were also analysed using ER-dsRed, Mito Tracker Red or Golgi-dsRed. **e**, Fractionation experiments confirm that STING resides in the ER. Control antibodies indicate accuracy of fractionation (Calreticulin, ER; COX IV, mitochondria; β-actin, cytosol).

We also established that while STING that had been tagged with HA at the carboxy region retained activity, this activity was lost when STING was tagged at the amino terminus or C terminus with GFP (data not shown). Subsequent analysis indicated that the N-terminal region of STING containing the five putative transmembrane regions (amino acids 1–230) or just the carboxyl region of STING (amino acids 173–379) did not exhibit significant ability, alone, to induce the IFN-β-Luc promoter (Fig. 2k, l). Thus, full length, intact STING is required for efficient function. However, we further observed that the carboxyl region of STING exerted a dominant-negative inhibitory effect and could impede the ability of full-length STING to stimulate IFN-β-Luc (Fig. 2m). Collectively, these data indicate that expression of STING activates the innate immune response, including type I IFN, leading to the induction of an antiviral state.

To further analyse STING function, we used an RNAi approach to ablate STING in a number of cell types. Our data indicated that knockdown of STING in HEK 293 cells modestly reduced the ability of the negative-stranded rhabdovirus VSV-GFP to induce IFN-β, presumably because these viruses are only weak activators of IFN-β (Supplementary Fig. 3). However, such cells were rendered extremely susceptible to virus infection and replication. To confirm a requirement for STING in the regulation of type I IFN induction and in host defence, we generated STING deficient (*Sting*$^{-/-}$) mice by targeted homologous recombination in embryonic stem (ES) cells (Supplementary Fig. 4). *Sting*$^{-/-}$ animals were born at the Mendelian ratio, and developed and bred normally. Accordingly, MEFs from wild-type and *Sting*$^{-/-}$ animals were infected with VSV-GFP at varying multiplicity of infection (m.o.i., 0.01–1) for up to 36 h post infection. This study confirmed that more progeny virus was produced in MEFs lacking STING compared to controls (by a factor of 10^2; 24–36 h) (Fig. 3a–d). These data was verified using VSV expressing a luciferase reporter gene and VSV-ΔM, which exhibits a defect in the viral matrix protein normally responsible for inhibiting cellular messenger RNA export from the nucleus[17](Supplementary Fig. 4 and Fig. 3e). Reconstitution of STING to *Sting*$^{-/-}$ MEFs rescued the susceptibility to VSV infection (Supplementary Fig. 4). Similar analysis also indicated that loss of STING also reduced the ability of Sendai virus to induce IFN-β (Fig. 3f). In contrast, we did not observe a strong requirement for STING to mediate the ability of transfected poly I:C to induce IFN-β induction, which is largely governed by the intracellular RIG-I homologue MDA5 (ref. 18) (Supplementary Fig. 5). We also observed that the positive-stranded encephalomyocarditis virus (EMCV), a member of the picornavirus family, did not effectively induce IFN-β or replicate differently, regardless of the presence of STING (Supplementary Fig. 5).

Thus we conclude that STING may play a more predominant role in facilitating RIG-I mediated innate signalling, rather than MDA5. Interestingly, we did notice a significant defect (>5-fold) in the ability of transfected B-form DNA (poly dA-dT) to induce IFN-β in MEFs lacking STING compared to controls (Fig. 3g, h). More strikingly, the non CpG containing interferon stimulatory DNA (ISD) was completely unable to induce IFN-β in *Sting*$^{-/-}$ MEFs, as were the DNA virus herpes simplex virus 1 and bacteria *Listeria monocytogenes* (Fig. 3i). TLR9 is considered to govern CpG DNA-mediated induction of IFN-β, but is not active in MEFs[19,20]. Thus, it is plausible that STING may function in TLR9-independent, DNA-mediated induction of type I IFN. This effect was similarly observed in murine STING-lacking bone marrow derived macrophages (BMDM) or bone marrow derived dendritic cells (GM-DC) cultured using granulocyte-monocyte colony stimulating factor (GM-CSF) (Supplementary Fig. 6). However, no significant difference was observed in the ability of exogenous poly I:C or lipopolysaccharide (LPS) to induce IFN-β, when comparing *Sting*$^{-/-}$ BMDMs or GM-DCs to controls, events which depend on TLR3 and TLR4, respectively. Whereas loss of STING rendered MEFs highly susceptible to VSV-GFP, less susceptibility was observed following VSV-GFP infection of *Sting*$^{-/-}$ GM-DCs or BMDMs, indicating that STING may be more important in facilitating negative-stranded virus-mediated innate signalling in fibroblasts. Collectively, our data indicate that loss of STING leads to a defect in RIG-I mediated type I IFN induction but does not affect the TLR pathway. In addition, we report that STING functions in the pathway used by intracellular B-form DNA to induce IFN-β.

To further examine the mechanisms of STING's function in innate signalling, we attempted to determine if STING interacted with RIG-I

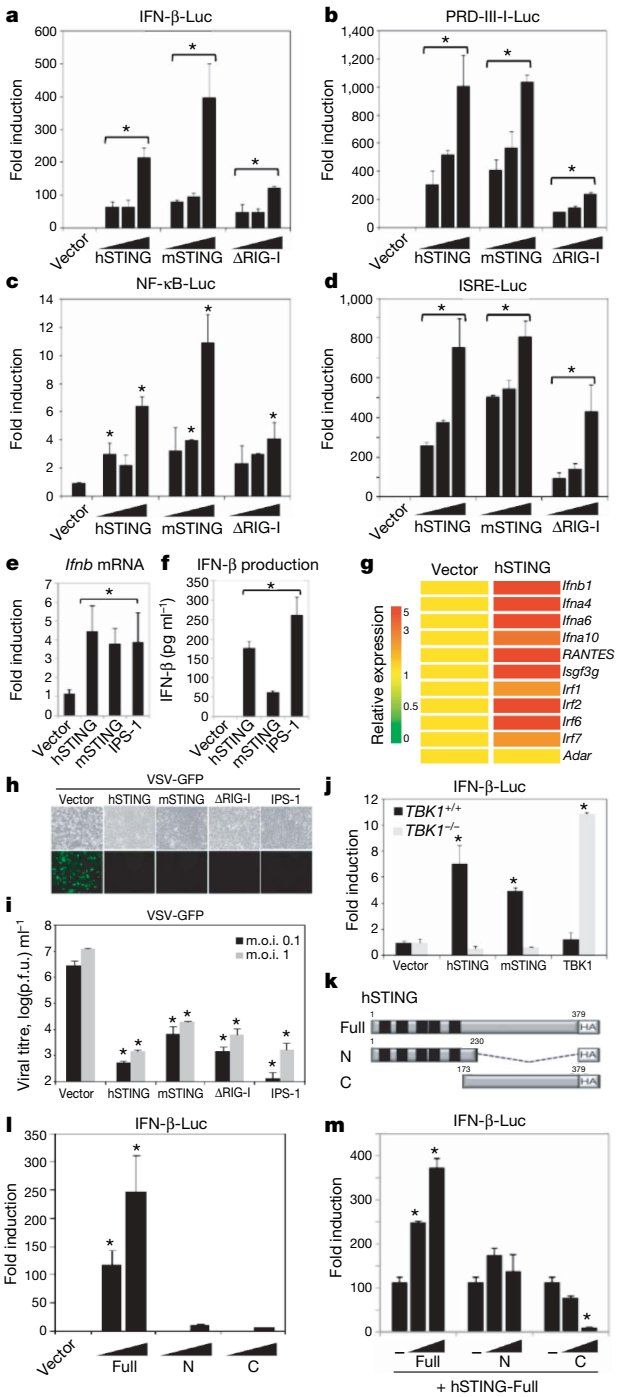

Figure 2 | STING facilitates IFN induction. **a**, 293T cells were transfected with an IFN-β-Luc (p110-Luc) plasmid and increasing amounts of human STING (hSTING), murine STING (mSTING) or control ΔRIG-I. **b**–**d**, 293T cells transfected as in **a** with either PRD-III-I-Luc (**b**), NF-κB-Luc (**c**) or ISRE-Luc (**d**) reporter plasmids were analysed similarly. **e**, MEFs were transfected as in **a**, and *Ifnb* mRNA was analysed by qRT–PCR. **f**, Medium from transfected MEFs was analysed for IFN-β protein by ELISA. **g**, Microarray analysis of 293T cells transfected with hSTING. **h**, MEFs transfected with STING or ΔRIG-I or IPS-1 are resistant to VSV-GFP infection (m.o.i., 1). Top panel is light microscopy, lower panel is fluorescent microscopy. **i**, Plaque assay from **h**. p.f.u., plaque-forming units. **j**, TBK-1 deficient MEFs do not facilitate STING signalling. **k**, Schematic of hSTING variants. **l**, 293T cells were transfected as in **a** with hSTING or variants, and luciferase measured. **m**, 293T cells were transfected with STING and increasing amounts of full length STING (hSTING-Full), hSTING-N or hSTING-C with luciferase plasmids as in **a**. Asterisks indicate significant difference ($P < 0.05$) as determined by Student's *t*-test. Error bars indicate s.d.

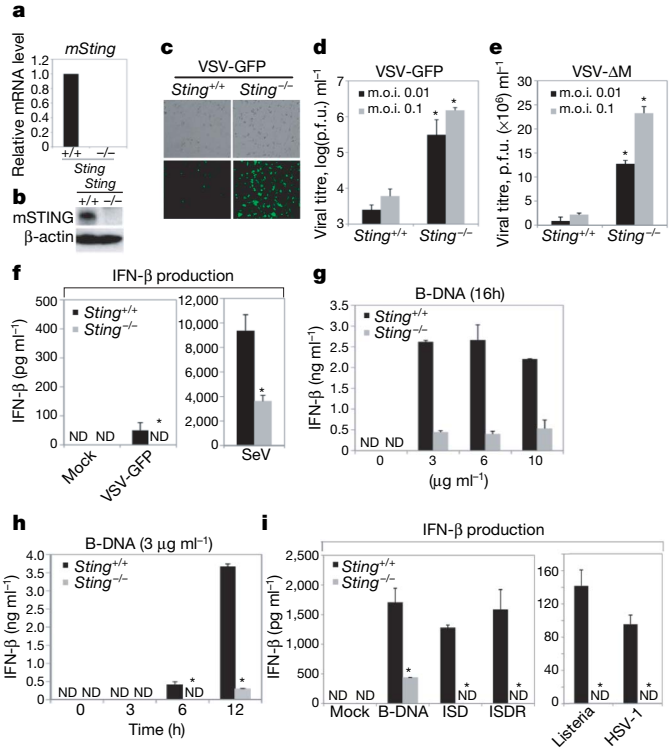

Figure 3 | Loss of STING affects host defence. **a**, qRT–PCR analysis of murine *Sting* mRNA in *Sting*$^{-/-}$ or control MEFs. **b**, Immunoblot of murine STING in −/− cells or controls. **c**, Fluorescence microscopy (GFP) of *Sting*$^{-/-}$ or controls infected with VSV-GFP (m.o.i., 0.1). **d**, Viral titres from **c**. **e**, Viral titres following VSV-ΔM infection. **f**, Endogenous IFN-β levels from *Sting*$^{-/-}$ or controls after infection with VSV-GFP (m.o.i., 1) or Sendai virus (SeV; m.o.i., 1). **g**, *Sting*$^{-/-}$ MEFs or controls were treated with transfected B-DNA and IFN-β measured by ELISA. **h**, Time-course analysis of **g**. **i**, *Sting*$^{-/-}$ or controls were exposed to transfected B-form DNA, interferon stimulatory DNA (ISD), ISD reversed nucleotide sequence (ISDR), *Listeria monocytogenes* (m.o.i. 50) and HSV-1 (m.o.i. 5) for 12 h, and IFN-β measured by ELISA. Asterisks indicate significant difference ($P < 0.05$) as determined by Student's *t*-test. Error bars indicate s.d. ND, not detectable.

and MDA5, which are putative innate immune signalling receptors for negative- or positive-stranded viral RNA, respectively[3,4,10]. Co-immunoprecipitation experiments in 293T cells principally indicated that FLAG-tagged RIG-I but not MDA5 could associate with HA-tagged STING in co-transfection experiments (Fig. 4a). The binding of RIG-I to STING was augmented upon infection of 293T cells with Sendai virus (Fig. 4a). We confirmed in normal human umbilical vein endothelial cells (HUVECs) that endogenous RIG-I could associate directly, or indirectly as a complex, with endogenous STING (Fig. 4b). This is in agreement with previous data indicating that STING seems to preferentially modulate the RIG-I, rather than the MDA5, regulated pathway (Fig. 3d and Supplementary Fig. 5). We also determined that the CARD domains of RIG-I (amino acids 1–284) were preferentially able to associate with HA-STING in transfected 293T cells (Fig. 4c). RIG-I was subsequently shown to colocalize with STING in the co-transfected 293T cells (Fig. 4d). It was similarly observed that the carboxyl region of STING could inhibit the function of RIG-I, again indicating that this region of STING can exhibit a dominant-inhibitory effect (Fig. 4e). We also noted association of the RIG-I downstream adaptor IPS-1 with STING although, similarly to the situation with RIG-I, it is not yet clear whether IPS-1 directly interacts with STING or exists as a complex with RIG-I/STING (Supplementary Fig. 7). Accordingly, we observed that STING was able to induce the expression of an IFN-β driven luciferase construct in MEFs lacking RIG-I or IPS-1, probably confirming that that STING functions downstream of these latter molecules

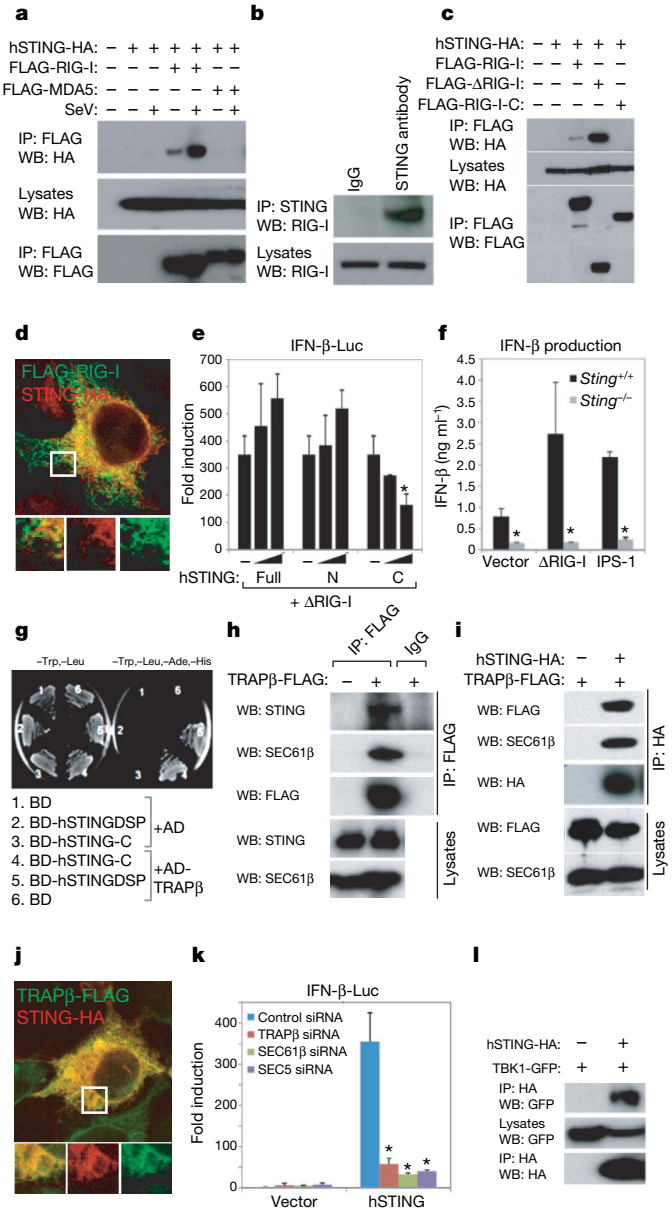

Figure 4 | STING associates with the translocon. **a**, 293T cells were co-transfected with HA-STING, FLAG-RIG-I or MDA5 and infected with Sendai virus (SeV; m.o.i. 1). Lysates were immunoprecipitated (IP) and immunoblotted (IB) using antibodies to HA or FLAG. **b**, Endogenous human STING associates with RIG-I in HUVECs. **c**, ΔRIG-I (amino acids 1–284) and not RIG-I-C (amino acids 218–925) associate with STING in co-transfected 293T cells. **d**, Confocal image of 293T cells co-transfected with tagged STING and RIG-I. **e**, 293T cells were co-transfected with control vector (−) or increasing amounts of full-length, amino (amino acids 1–230) or carboxyl (amino acids 173–379) STING and ΔRIG-I, and IFN-β-Luc was measured. **f**, Control or *Sting*$^{-/-}$ MEFs were transfected with ΔRIG-I (amino acids 1–284) or IPS-1 and IFN-β was measured by ELISA. **g**, GAL4 binding domain (BD) fused to the carboxyl region of hSTING, BD-hSTING-C, interacts with Ssr2/TRAPβ fused to the GAL4 activation domain (AD-hTRAPβ) in yeast-two hybrid screening (BD-hSTINGΔSP, amino acids 36–369; BD-hSTING-C, amino acids 173–379). **h**, HEK 293 cells were transfected with FLAG-tagged TRAPβ and endogenous STING or SEC61β measured by immunoblot. **i**, STING and TRAPβ were co-transfected HEK 293 cells and analysis carried out as in **h**. **j**, Co-localization of STING and TRAPβ in 293T cells. **k**, RNAi to TRAPβ, SEC61β or SEC5 in HEK 293 cells ablates STING signalling. **l**, HA-STING associates with GFP-TBK-1 in co-transfected HEK 293 cells. Asterisks indicate significant difference ($P < 0.05$) as determined by Student's *t*-test. Error bars indicate s.d.

(Supplementary Fig. 8). The ability of ΔRIG-I or IPS-1 to induce IFN-β appeared diminished in *Sting*$^{-/-}$ MEFs (Fig. 4f). However, there was also a marked reduction in the induction of IFN-β by all transfected plasmids (including vector alone) in the absence of STING compared to control MEFs, probably because endogenous DNA innate signalling pathways are defective (Fig. 3g–i). These data indicate that STING may be an important downstream adaptor molecule that facilitates RIG-I and perhaps IPS-1 function.

To gain further insight into the molecular mechanisms of the action of STING, we screened an IFN-induced, human fibroblast yeast two-hybrid cDNA library using STING (amino acids 173–379) as a bait and repeatedly isolated SSR2/TRAPβ, a member of the TRAP complex comprising four subunits (α–Δ) that facilitates translocation of proteins into the ER following translation (Fig. 4g)[1,2]. The TRAP complex is known to associate with the translocon, comprising three subunits, SEC61α, SEC61β and SEC61γ. Given this information, we confirmed that TRAPβ can indeed associate with endogenous STING in HEK 293 cells following co-immunoprecipitation experiments (Fig. 4h). Using this approach, we confirmed that TRAPβ also co-immunoprecipitated with endogenous SEC61β (Fig. 4h). We next verified that STING could also associate not only with TRAPβ but also SEC61β, probably as a complex (Fig. 4i). STING was also observed to colocalize with TRAPβ in the ER region of the cell (Fig. 4j). Indeed, loss of TRAPβ or SEC61β reduced STING's ability to induce an IFN-β promoter driving luciferase (Fig. 4k; Supplementary Fig. 9). Taken together, these data indicate that the STING may be involved in translocon function, and that the translocon may be able to influence the induction of type I IFN.

Thus, STING is predominantly an ER resident protein that may link RIG-I and DNA-mediated intracellular innate signalling to the translocon. We speculate that RIG-I may detect translating viral RNAs at the intersection of ribosome/ER translocon association and require STING to exert effective function[2]. Alternatively, STING may participate in mediating ER stress response pathways, but this remains to be verified. Although it is not clear how signalling from the translocon to IRF3/NF-κB occurs, it has recently been established that the translocon physically associates with the exocyst—the octameric Sec6–Sec8 complex that also associates with the ER and tethers secretory vesicles to membranes, and facilitates protein synthesis and secretion[21,22]. Recently, the exocyst complex was found to recruit and activate TBK1 and play a role in type I IFN-β induction[23]. Our preliminary analysis indicates that STING also co-immunoprecipitates with TBK1, and that RNAi ablation of Sec5 also rendered cells defective in the STING function (Fig. 4k, l). Thus STING may facilitate the detection of intracellular viral RNA species as well as B-form DNA, indicating convergence of these intracellular PAMP recognition pathways.

METHODS SUMMARY

Plasmid constructs. Human STING (hSTING), murine STING (mSTING), hSTING-N (amino acids 1–230) and hSTING-C (amino acids 173–379) sequences were amplified by PCR and were cloned into pcDNA3 plasmids to generate C-terminally HA-tagged expression constructs. Expression plasmids encoding Flag-tagged RIG-I, ΔRIG-I (amino acids 1–284), IPS-1 and TBK-1 were described previously[24]. GFP-tagged RIG-I and TBK-1 were generated by cloning into pAcGFP1-C1 (Clontech). Other plasmids were obtained as follows: p110-Luc and PRD-III-I-Luc (T. Maniatis), IFN-β-Luc and ISRE-Luc (J. Hiscott), NFκB-Luc (Stratagene), ER-dsRED and Golgi-dsRED (Clontech).

Antibodies. Rabbit polyclonal antibody against a synthetic peptide corresponding to residues 324–340 of human STING was obtained from EvoQuest Custom Antibody Services (Invitrogen). Other antibodies were obtained from following sources: SEC61β (Upstate), β-Actin, HA, FLAG (Sigma), COX IV, Calreticulin, IRF3 and RIG-I (Abcam).

Confocal microscopy. ER-dsRED and Golgi-dsRED (Clontech) were used for ER and Golgi marker, respectively. For mitochondria staining, living cells were incubated with 300 nM of Mito Tracker Red (Invitrogen) for 45 min at 37 °C.

RNA interference. Chemically synthesized 21-nucleotide siRNA duplexes were obtained from Dharmacon. RNA oligonucleotides used for human and murine STING were as follows: hSTING, GCAUCAAGGAUCGGGUUU; mSTING, CCAACAGCGUCUACGAGA.

Generation of the *Sting* knockout mice. The linearized targeting vector was electroporated into E14.1 ES cells originated from 129SvEv strain, followed by the selection in G418. One positive clone was injected into C57BL/6J blastocysts and $Sting^{-/-}$ mice generated on a C57BL/6J background.

Yeast two-hybrid analyses. To screen for interacting partners of STING, a yeast two-hybrid approach was used, adopting a novel IFN-induced, telomerase immortalized human fibroblast cDNA library, generated by our laboratory. hSTING-C (amino acids 173–379) sequence was amplified by PCR and was cloned into pGBK-T7 (Clontech) to generate a bait plasmid pGBK-T7-hSTING-C. 100 μg of the IFN-induced library's plasmid DNA was used to perform a library-scale transformation of yeast strain Y187.

Statistics. Students *t*-test was used to analyse data.

Full Methods and any associated references are available in the online version of the paper at www.nature.com/nature.

Received 7 July; accepted 6 August 2008.
Published online 24 August 2008.

1. Hartmann, E. *et al.* A tetrameric complex of membrane proteins in the endoplasmic reticulum. *Eur. J. Biochem.* **214,** 375–381 (1993).
2. Menetret, J. F. *et al.* Architecture of the ribosome-channel complex derived from native membranes. *J. Mol. Biol.* **348,** 445–457 (2005).
3. Takeuchi, O. & Akira, S. Recognition of viruses by innate immunity. *Immunol. Rev.* **220,** 214–224 (2007).
4. Beutler, B. *et al.* Genetic analysis of resistance to viral infection. *Nature Rev. Immunol.* **7,** 753–766 (2007).
5. Takahasi, K. *et al.* Nonself RNA-sensing mechanism of RIG-I helicase and activation of antiviral immune responses. *Mol. Cell* **29,** 428–440 (2008).
6. Pichlmair, A. *et al.* RIG-I-mediated antiviral responses to single-stranded RNA bearing 5′-phosphates. *Science* **314,** 997–1001 (2006).
7. Hornung, V. *et al.* 5′-Triphosphate RNA is the ligand for RIG-I. *Science* **314,** 994–997 (2006).
8. Yoneyama, M. *et al.* The RNA helicase RIG-I has an essential function in double-stranded RNA-induced innate antiviral responses. *Nature Immunol.* **5,** 730–737 (2004).
9. Loo, Y. M. *et al.* Distinct RIG-I and MDA5 signaling by RNA viruses in innate immunity. *J. Virol.* **82,** 335–345 (2008).
10. Onomoto, K., Yoneyama, M. & Fujita, T. Regulation of antiviral innate immune responses by RIG-I family of RNA helicases. *Curr. Top. Microbiol. Immunol.* **316,** 193–205 (2007).
11. Kawai, T. *et al.* IPS-1, an adaptor triggering RIG-I- and Mda5-mediated type I interferon induction. *Nature Immunol.* **6,** 981–988 (2005).
12. Meylan, E. *et al.* Cardif is an adaptor protein in the RIG-I antiviral pathway and is targeted by hepatitis C virus. *Nature* **437,** 1167–1172 (2005).
13. Seth, R. B. *et al.* Identification and characterization of MAVS, a mitochondrial antiviral signaling protein that activates NF-kappaB and IRF 3. *Cell* **122,** 669–682 (2005).
14. Xu, L. G. *et al.* VISA is an adapter protein required for virus-triggered IFN-beta signaling. *Mol. Cell* **19,** 727–740 (2005).
15. McWhirter, S. M. *et al.* IFN-regulatory factor 3-dependent gene expression is defective in Tbk1-deficient mouse embryonic fibroblasts. *Proc. Natl Acad. Sci. USA* **101,** 233–238 (2004).
16. Balachandran, S., Thomas, E. & Barber, G. N. A FADD-dependent innate immune mechanism in mammalian cells. *Nature* **432,** 401–405 (2004).
17. Faria, P. A. *et al.* VSV disrupts the Rae1/mrnp41 mRNA nuclear export pathway. *Mol. Cell* **17,** 93–102 (2005).
18. Kato, H. *et al.* Differential roles of MDA5 and RIG-I helicases in the recognition of RNA viruses. *Nature* **441,** 101–105 (2006).
19. Ishii, K. J. *et al.* A Toll-like receptor-independent antiviral response induced by double-stranded B-form DNA. *Nature Immunol.* **7,** 40–48 (2006).
20. Stetson, D. B. & Medzhitov, R. Recognition of cytosolic DNA activates an IRF3-dependent innate immune response. *Immunity* **24,** 93–103 (2006).
21. Guo, W. & Novick, P. The exocyst meets the translocon: A regulatory circuit for secretion and protein synthesis? *Trends Cell Biol.* **14,** 61–63 (2004).
22. Lipschutz, J. H., Lingappa, V. R. & Mostov, K. E. The exocyst affects protein synthesis by acting on the translocation machinery of the endoplasmic reticulum. *J. Biol. Chem.* **278,** 20954–20960 (2003).
23. Chien, Y. *et al.* RalB GTPase-mediated activation of the IkappaB family kinase TBK1 couples innate immune signaling to tumor cell survival. *Cell* **127,** 157–170 (2006).
24. Balachandran, S. *et al.* Fas-associated death domain-containing protein-mediated antiviral innate immune signaling involves the regulation of Irf7. *J. Immunol.* **178,** 2429–2439 (2007).

Supplementary Information is linked to the online version of the paper at www.nature.com/nature.

Acknowledgements We thank T. Venkataraman, J. Hyun, T. Sato and M. Conkright for technical assistance, M. Gale for RIG-I and IPS-1 lacking MEFs, Y. C. Weh for TBK-1 lacking MEFs, and S. Nagata, T. Maniatis, J. Hiscott and N. Reich for plasmid constructs.

Author Information Reprints and permissions information is available at www.nature.com/reprints. Correspondence and requests for materials should be addressed to G.N.B. (gbarber@med.miami.edu).

METHODS

Cells, viruses and reagents. 293T and HEK293 cells were obtained from the ATCC and were maintained in DMEM medium supplemented with 10% FBS. Human umbilical vein endothelial cells (HUVECs) were obtained from Lonza, and were maintained in endothelial growth medium, EGM-2 (Lonza). *Fadd*$^{+/+}$, *Fadd*$^{-/-}$, *Tbk-1*$^{+/+}$ and *Tbk-1*$^{-/-}$ MEFs were provided by W.-C. Yeh[16]. VSV-GFP was used in infections and titred as described[16]. VSV-ΔM was constructed as described[17]. Murine IFN-β ELISA Kit was obtained from PBL. EMCV was purchased from ATCC. Synthetic ds B-DNA (poly dA-dT) and poly I:C were purchased from GE Healthcare. Interferon stimulatory DNA (ISD) and reverse sequence of ISD were described previously[20]. For stimulation of cells, B-DNAs or poly I:C were mixed with Lipofectamine 2000 (Invitrogen) at a ratio of 1:1 (vol/wt), and then added to cells at a final concentration of 3 μg ml^{-1}.

Reporter analysis. 293T cells or MEFs seeded on 24-well plates were transiently transfected with 50 ng of the luciferase reporter plasmid together with a total of 250 ng of various expression plasmids or empty control plasmids. As an internal control, 10 ng of pRL-TK was transfected simultaneously. Then, 36 h later, the luciferase activity in the total cell lysates was measured.

Northern blot. Human multiple tissue RNA blots (Clontech) were hybridized with a ^{32}P-labelled full-length human STING probe.

Real-time PCR. Total RNA was isolated from cells using the RNeasy RNA extraction kit (Qiagen) and cDNA synthesis was performed using 1 μg of total RNA (Roche). Fluorescence real-time PCR analysis was performed using a LightCycler 2.0 instrument (Roche Molecular Biochemicals) and TaqMan Gene Expression Assays (Applied Biosystems). Relative amounts of mRNA were normalized to the 18S ribosomal RNA levels in each sample.

DNA microarray analysis. Total RNA was extracted from 293T cells transfected with STING expressing vectors. Preparation of cDNA and microarray analysis was performed at the W.M. Keck Foundation Biotechnology Research Laboratory DNA microarray facility at Yale University. The Human Genome U133 Plus 2.0 Array (Affymetrix) was used. Data analysis was performed with GeneSpring software (Silicon Genetics)[16].

Mitochondria and ER fraction isolation. Mitochondria and ER membranes were purified on discontinuous sucrose gradients as previously described[25]. Briefly, HUVEC cells in MTE buffer (0.27 M mannitol, 10 mM Tris-HCl, 0.1 mM EDTA, pH 7.4) were lysed by sonication. Lysed cells were centrifuged at 700*g* for 10 min to remove nuclei and cellular debris. Mitochondria were obtained by centrifugation at 15,000*g* for 10 min, and post mitochondrial supernatant was used for purification of ER fractions. Mitochondria pellet was resuspended in MTE buffer, and was layered on discontinuous sucrose gradients consisting of 1.0 M and 1.7 M sucrose and banded by centrifugation at 40,000*g* for 22 min. Mitochondria fraction was collected and pelleted by centrifugation at 15,000*g* for 10 min. Purified mitochondria were resuspended in PBS and used for western blot analysis. To isolate ER fractions, postmitochondrial supernatant described above was layered on discontinuous sucrose gradients consisting of 1.3 M, 1.5 M and 2.0 M sucrose, and banded by centrifugation at 100,000*g* for 70 min. The ER fraction at the interface between the supernatant and the 1.3 M sucrose was collected, and pelleted by centrifugation at 100,000*g* for 45 min. The ER membranes were resuspended in PBS and were used for western blot analysis.

RNA interference. 93T cells were plated on 24-well plates at 5×10^4 cells per well and transfected with 10 pmol of siRNA duplex per well using Lipofectamine RNAiMAX (Invitrogen). MEFs were transfected by using an Amaxa nucleofector apparatus (program A-023) and Amaxa MEF nucleofector kit 1 according to the manufacturer's recommendations. At 72 h after transfection, cells were used for further experiments.

Primers. The following primers were used for cloning: hSTING forward, 5′-CCCAAGCTTGCCGCCACCATGCCCCACTCCAGCCTGC-3′; hSTING reverse, 5′-CCCAAGCTTGCCGCCACCATGCCATACTCCAACCTGCATCC-3′; mSTING forward, CCGCTCGAGAGAGAAATCCGTGCGGAGAG; mSTING reverse, CCGC TCGAGGATGAGGTCA.

The sequences of each siRNA oligonucleotide used in this study are follows: hSTING siRNA, 5′-GCAUCAAGGAUCGGGUUU-3′; mSTING siRNA, 5′-CCAACAGCGUCUACGAGA-3′; SSR2 siRNA, 5′-UCUCAAGGCUGGUU AUUU-3′, 5′-GUGGAACUAUCUGAUGAU-3′, 5′-CAUCUACAAUGUUG GCUC-3′, 5′-AAACGAAGAAGAACUGAU-3′; hSEC61B siRNA, 5′-CAGUA UUGGUUAUGAGUC-3′; 5′-GUUCGUAGAUUCAGUUAC-3′, 5′-GCUCA AAGUUGGCCCUGU-3′, 5′-CUGUAAGCUUGCUGUUUU-3′; SEC5 siRNA, 5′-CGUCACACCUUCCUAAAU-3′, 5′-CGGCAUCUCUCCAAAUGA-3′, 5′-CAACAGGUGUCAGAAACU-3′, 5′-GAAAGGCGGUCUCAGUAC.

Co-immunoprecipitation, native PAGE and immunoblot analysis. Cells were seeded on 100-mm dishes at 1×10^6 cells per dish. Cells were transfected with a total of 10 μg of empty plasmid or various expression plasmids using Lipofectamine 2000. At 36 h after transfection, cells were lysed in M-PER buffer (Pierce) or 1% digitonin (Calbiochem) buffer (20 mM Tris-HCl, 150 mM NaCl, 1% digitonin) containing protease inhibitors (Roche). Lysates were incubated with HA affinity matrix (Covance) or FLAG affinity beads (Sigma) overnight. The beads were washed three times by TBS containing 0.05% Tween-20 and immunoprecipitates were eluted with non-reducing sample buffer by boiling for 5 min. For endogenous STING immunoprecipitation, HUVECs were lysed in 1% digitonin lysis buffer. Cleared supernatants were incubated with 10 μg of anti-STING antibody, followed by incubation with immobilized protein G (Pierce). The beads were washed four times by 1% digitonin lysis buffer and immunoprecipitates were eluted with SDS sample buffer by boiling for 5 min. Native PAGE and immunoblotting was carried out as previously described[24].

Generation of the *Sting* knockout mice. The linearized targeting vector was electroporated into E14.1 ES cells originated from 129SvEv strain, followed by the selection in G418. Targeted clones were screened by PCR. From 90 clones, 1 positive clone was identified. This ES clone was subjected to the generation of chimaera mice by injection using C57BL/6J blastocysts as the host. The resulting male chimaeras were further mated with C57BL/6J female mice for germline transmission. The heterozygous mice (F_1 mice) were interbred to obtain wild-type, heterozygous and homozygous littermates (F_2). The genotypes of the mice were determined by PCR. Animals were bred at the University of Miami School of Medicine Transgenic Core Facility. Mice were allowed to freely access to food and water and housed at an ambient temperature of 23 °C and at a 12 h light/dark cycle. Animal care and handling was performed as per IACUC guidelines.

IFN induced library construction. To screen for interacting partners of STING, a yeast two hybrid approach was adopted using a novel IFN-induced, telomerase immortalized human fibroblast cDNA library. To construct this library, cells were treated overnight with 1,000 units each of human IFN-α and -β to induce interferon dependent genes. Poly(A)$^+$ RNA was extracted and cDNA synthesis was carried out using BD Powerscript RT (Clontech). The cDNA was then amplified by PCR, digested with *SfiI* and ligated to the yeast prey vector pGADT7-RecAB. The ligated mixture was transformed into *Escherichia coli* strain DH10B. The number of independent clones in the unamplified library was estimated to be 3.2×10^6, with an average size of 1.52 kb and inserts ranging in size from 0.8 to 3.0 kb. 15 independent colonies were isolated and DNA extracted to check for size by PCR.

25. Mavinakere, M. S. *et al.* Processing of human cytomegalovirus UL37 mutant glycoproteins in the endoplasmic reticulum lumen prior to mitochondrial importation. *J. Virol.* **80**, 6771–6783 (2006).

CORRIGENDUM

doi:10.1038/nature07347

The delayed rise of present-day mammals

Olaf R. P. Bininda-Emonds, Marcel Cardillo, Kate E. Jones, Ross D. E. MacPhee, Robin M. D. Beck, Richard Grenyer, Samantha A. Price, Rutger A. Vos, John L. Gittleman & Andy Purvis

Nature 446, 507–512 (2007)

We have discovered a bug in the Perl script relDate v.2.2 that was used in part to date the nodes in the species-level mammalian supertree presented and analysed in our Article. The bug affected all but 80 of the 2,109 published dates, generally causing them to be slightly inflated, with the effect being stronger in more recent nodes. The absolute errors are mostly small (mean and median change of 1.32 and 0.70 million years, respectively), and a strong correlation between the two sets of dates exists ($r = 0.990$); however, 25 dates (all within Chiroptera) do change by more than 10 million years. Four of these dates are associated with the paraphyletic genus *Hipposideros*, whereas the remaining 21 cover most of Molossidae. The errors do not affect the results or overall conclusions of our paper qualitatively.

The Supplementary Information, including the tree files, has now been amended and can be accessed through the Supplementary Information link of the original Article. An additional file with a version of the amended Article can be accessed at http://www.uni-oldenburg.de/molekularesystematik/ under the 'Publikationen/ Publications' link.

CORRIGENDUM

doi:10.1038/nature07432

STING is an endoplasmic reticulum adaptor that facilitates innate immune signalling

Hiroki Ishikawa & Glen N. Barber

Nature 455, 674–678 (2008)

We inadvertently failed to notice that STING protein is encoded by the same gene as the previously described plasma membrane tetraspanner MPYS[1].

1. Jin, L. *et al.* MPYS, a novel membrane tetraspanner, is associated with major histocompatibility complex cass II and mediates transduction of apoptotic signals. *Mol. Cell. Biol.* 28, 5014–5026 (2008).

CORRIGENDUM

doi:10.1038/nature07514

A role for clonal inactivation in T cell tolerance to Mls-1[a]

Marcia A. Blackman, Hans-Gerhard Burgert, David L. Woodland, Ed Palmer, John W. Kappler & Philippa Marrack

Nature 345, 540–542 (1990)

In this Article, the name of Hans-Gerhard Burgert was incorrectly listed as Hans Gerhard-Burgert.

ADDENDUM

doi:10.1038/nature07566

Genes mirror geography within Europe

John Novembre, Toby Johnson, Katarzyna Bryc, Zoltán Kutalik, Adam R. Boyko, Adam Auton, Amit Indap, Karen S. King, Sven Bergmann, Matthew R. Nelson, Matthew Stephens & Carlos D. Bustamante

Nature 456, 98–101 (2008)

A related manuscript arriving at broadly similar conclusions based on partially overlapping data has recently been published[1]. Specifically, 661 of the 3,192 samples from the POPRES collection[2] analysed in our paper were also analysed by Lao *et al.*[1].

1. Lao, O. *et al.* Correlation between genetic and geographic structure in Europe. *Curr. Biol.* 18, 1241–1248 (2008).
2. Nelson, M. R. *et al.* The population reference sample, POPRES: a resource for population, disease, and pharmacological genetics. *Am. J. Hum. Genet.* 83, 347–358 (2008).

CORRIGENDUM

doi:10.1038/nature07515

Structural basis for specific cleavage of Lys 63-linked polyubiquitin chains

Yusuke Sato, Azusa Yoshikawa, Atsushi Yamagata, Hisatoshi Mimura, Masami Yamashita, Kayoko Ookata, Osamu Nureki, Kazuhiro Iwai, Masayuki Komada & Shuya Fukai

Nature 455, 358–362 (2008)

In this Fig. 3c of this Article, Asp 324 was incorrectly labelled as Glu 324.